JOURNAL OF AGRICULTURAL AND FOOD CHEMISTRY

Stability of Chitosan Nanoparticles for L-Ascorbic Acid during Heat Treatment in Aqueous Solution

KEUM-IL JANG[†] AND HYEON GYU LEE*[,‡]

Department of Food Science and Technology, Chungbuk National University, 12 Gaeshin-dong, Heungduk-gu, Cheong-Ju, Chungbuk 361-763, South Korea, and Department of Food and Nutrition, Hanyang University, 17 Haengdang-dong, Seongdong-gu, Seoul 133-791, South Korea

This study investigated the stability and characteristics of L-ascorbic acid (AA)-loaded chitosan (CS) nanoparticles during heat processing in aqueous solutions. AA-loaded CS nanoparticles were prepared by ionic gelation of CS with tripolyphosphate (TPP) anions. The smallest CS nanoparticles (170 nm) were obtained with a CS concentration of 1.5 mg/mL and a TPP concentration of 0.6 mg/mL. As the concentration of AA increased from 0.1 to 0.3 mg/mL, the particle size increased, while the zeta potential decreased, and the encapsulation efficiency of AA remained within a fixed range (10–12%). During heat processing at various temperatures, the size and zeta potential of the particles decreased rapidly in the first 5 min and then slowly fell to the regular range. At the beginning of the release profiles, the burst release-related stability of the surface increased with the temperature. Then, the release of the internal AA was constantly higher with a longer release time. Consequently, it was confirmed that the stability of AA-loaded CS nanoparticles was affected by temperature but that the internal stability was greater than the surface stability. These results demonstrate the stability of CS nanoparticles for AA during heat processing and suggest the possible use of AA-loaded CS nanoparticles to enhance antioxidant effects because of the continuous release of AA from CS nanoparticles in food processing.

KEYWORDS: Ascorbic acid; chitosan nanoparticle; heat stability; ionic gelation; release

INTRODUCTION

The cationic polyelectrolyte chitosan (CS) is the second most abundant polysaccharide present in nature. CS has shown favorable biocompatibility characteristics (*1–3*), as well as the ability to increase membrane permeability, both in vitro (*4–6*) and in vivo (*7*), and can be degraded by lysozyme in serum. CS is similar in structure to cellulose; both are made from linear β-(1→4)-linked monosaccharides. However, unlike cellulose, CS is composed of 2-amino-2-deoxy-β-D-glucan combined with glycosidic linkages. The primary amine groups give CS special properties that make it very useful in pharmaceutical applications. Compared to many other natural polymers, CS has a positive charge and is mucoadhesive (*8*).

As CS is a cationic polysaccharide in neutral or basic pH conditions, it contains free amino groups and, hence, is insoluble in water. At acidic pH, amino groups can undergo protonation, thus making them soluble in water (*9*). Solubility of CS depends on the distribution of free amino and *N*-acetyl groups. Protonation of the amino group allows the polymer to interact with negatively charged materials (*10*). It is this functional group that enables the formation of CS nanoparticles cross-linked with anion materials, such as sodium tripolyphosphate (TPP), by the ionic gelation method (*11, 12*).

CS nanoparticles have been synthesized as constituent nonviral carriers for the delivery of peptides, proteins, oligonucleotides, vitamins, plasmids, and drugs (*13*). They have the capacity to protect sensitive bioactive macromolecules from enzymatic and chemical degradation in vivo and during storage (*14*) and facilitate the transport of charged macromolecules across absorptive epithelial cells (*15*). Insulin-loaded CS nanoparticles could enhance intestinal absorption of insulin and increase its relative pharmacological bioavailability (*16*). CS nanoparticles have been employed as gene carriers to enhance gene transfer efficiency into cells (*17*). CS microspheres have also been used for gastric drug delivery, and reacetylated CS microspheres have been prepared for controlled release of active antimicrobial agents, such as amoxycillin and metronidazole into the gastric cavity (*18*).

L-Ascorbic acid (AA), commonly known as vitamin C, is a representative water-soluble vitamin that has a variety of biological, pharmaceutical, and dermatological functions. It promotes collagen biosynthesis, provides photoprotection, causes melanin reduction, scavenges free radicals, and enhances immunity. These functions are closely related to the well-known antioxidant properties of this compound in foodstuffs, cosmetics, and pharmaceutical preparations (*19–21*). However, AA is very unstable in air, oxygen, light,

* Corresponding author (telephone +82-2-2220-1202; fax +82-2-2292-1226; email hyeonlee@hanyang.ac.kr).
[†] Chungbuk National University.
[‡] Hanyang University.

10.1021/jf073385e CCC: $40.75
Published on Web 02/20/2008

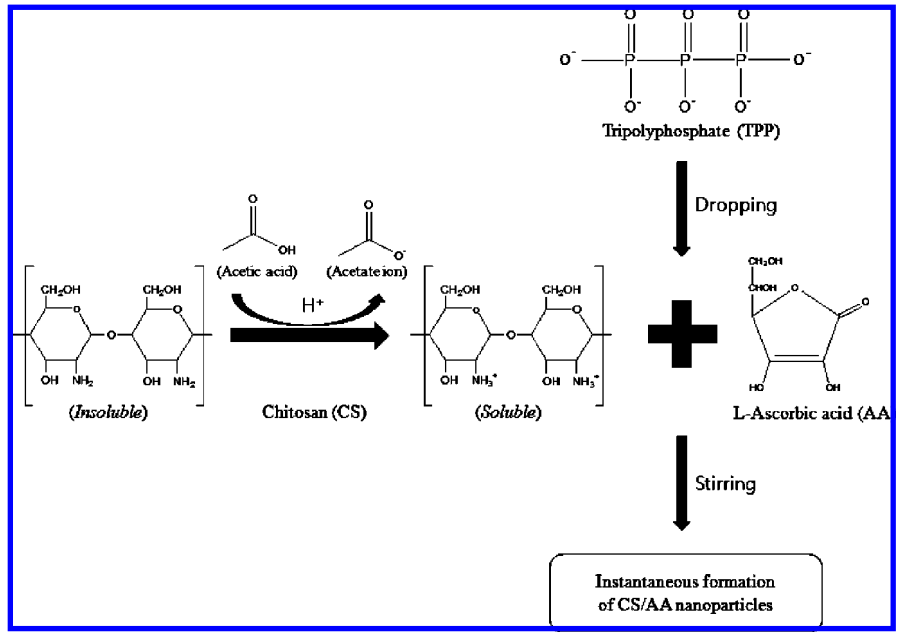

Figure 1. Scheme of the preparation of CS/AA nanoparticles.

and moist conditions, at high temperatures, with metal ions, and in food processing, during which it easily decomposes into biologically inactive compounds such as 2,3-diketo-L-gulonic acid, oxalic acid, L-threonic acid, L-xylonic acid, and L-lyxonic acid (*22–24*). The degradation of AA is a major cause of quality and color changes during processing and storage of food products. To overcome some of these shortcomings of AA, the nanoparticle technique may be suitable for maintenance of AA bioactivity. However, the use of AA-loaded CS nanoparticles and the heat stability of CS nanoparticles have seldom been reported.

The aim of this study was to investigate the stability and characteristics of AA-loaded CS nanoparticles during heat processing in aqueous solutions. For this purpose, we first prepared the CS nanoparticles and AA-loaded CS nanoparticles on the basis of the ionic gelation of CS with TPP anions. Then, we investigated the unique characteristics of AA-loaded CS nanoparticles in terms of particle size, zeta potential, encapsulation efficiency (EE), and release effects. Finally, we evaluated the stability of AA-loaded CS nanoparticles with the changes of physicochemical properties and release rate before and after heat processing in aqueous solutions at various temperatures.

MATERIALS AND METHODS

Materials. CS with a deacetylation degree (DD) of 86.6% and low molecular weight (catalog no. LMW 448869) and sodium TPP were purchased from Sigma-Aldrich Chemical Co. (Sigma, St. Louis, MO) (*25*). Sodium L-ascorbate was obtained from the Kanto Chemical Co. (Tokyo, Japan), and acetic acid was purchased from Shinyo Pure Chemistry (Osaka, Japan).

Preparation of CS Nanoparticles and AA-Loaded CS Nanoparticles. CS nanoparticles were prepared according to the procedure reported by Calvo et al. (*12*) and Wu et al. (*26*) based on the ionic gelation of CS with TPP anions. The scheme for the prepration of CS nanoparticles is shown in **Figure 1**. CS was dissolved in acetic acid aqueous solution at various concentrations (2.4, 3.2, 4.0, and 4.8 mg/mL). The concentration of acetic acid in aqueous solution was, in all cases, 1.75 times that of CS. Under magnetic stirring (400 rpm) at room temperature, 3 mL of TPP aqueous solutions at various concentrations (1.33, 1.60, and 1.47 mg/mL), was added into 5 mL of CS solutions using a peristaltic pump with a 1 mL/min flow rate. The final concentrations of CS and TPP in nanoparticle suspensions were 1.5, 2.0, 2.5, and 3.0 mg/mL and 0.5, 0.6, and 0.7 mg/mL, respectively. The concentration of acetic acid in aqueous solution was, in all cases, 1.75 times the final concentration of CS. For the association of AA with CS nanoparticles, sodium ascorbate was dissolved in distilled water. Under magnetic stirring, the AA-loaded CS nanoparticles were formed by addition of 3 mL of TPP solution (0.6 mg/mL) into 5 mL of CS solution (1.5 mg/mL) containing sodium ascorbate (0.1, 0.2, and 0.3 mg/mL) using a peristaltic pump at 1 mL/min flow rate.

Physicochemical Properties of CS Nanoparticles and AA-Loaded CS Nanoparticles. The particle sizes and zeta potentials of the CS nanoparticles and AA-loaded CS nanoparticles were measured with a Malvern Zetasizer Nano ZS (Malvern Instruments Ltd., Malvern, U.K.), respectively. The particle size distribution of the nanoparticles is reported as a polydispersity index (PDI). All measurements were performed in triplicate.

AA Encapsulation Efficiency into CS Nanoparticles. The EE of AA-loaded CS nanoparticles was determined by the separation of nanoparticles from the aqueous medium containing nonassociated AA using ultracentrifugation (Optima TL Ultracentrifuge, Beckman, Fullerton, CA) at 15000*g*, 4 °C and vacuum condition for 30 min. The amount of free AA in the supernatant was measured by high-performance liquid chromatography (HPLC, Thermo Separation Products, Waltham, MA). A 250 × 4.6 mm column (C_{18} column; Thermo Separation Products) was used as the solid phase. The mobile phase consisted of 50 mM potassium dihydrogen phosphate and acetonitrile at a ratio of 6:4 (*27, 28*). The flow rate was 1 mL/min, and the detection wavelength of the UV detector (Spectra System UV1000; Thermo Separation Products) was set at 244 nm for the ascorbic acid solution (*22*). An injection volume of 20 μL was delivered using an autosampler (Spectra System AS1000; Thermo Separation Products), and quantitation was done via electronic integration of the peak area using MultiChro version 5.0 (Yullin Technology, Seoul, Korea). All measurements were performed in triplicate. The EE of AA into the nanoparticles was calculated as

$$EE = (A - B)/A \times 100 \quad (1)$$

where A is total AA and B is free AA.

In Vitro Release of AA from CS Nanoparticles. AA-loaded CS nanoparticles were separated by centrifugation at 15000*g*, 4 °C and vacuum condition for 30 min. The supernatant was decanted, and the nanoparticles were resuspended in 4 mL of 0.26% acetic acid solution in distilled water and then kept at 37 °C for 4 days. Each day, 0.5 mL of the suspension was filtered though a 0.22 μm syringe filter (Millipore Co., Bedford, MA), and the AA concentrations in the supernatant were analyzed by HPLC. The HPLC method for the AA content in acetic

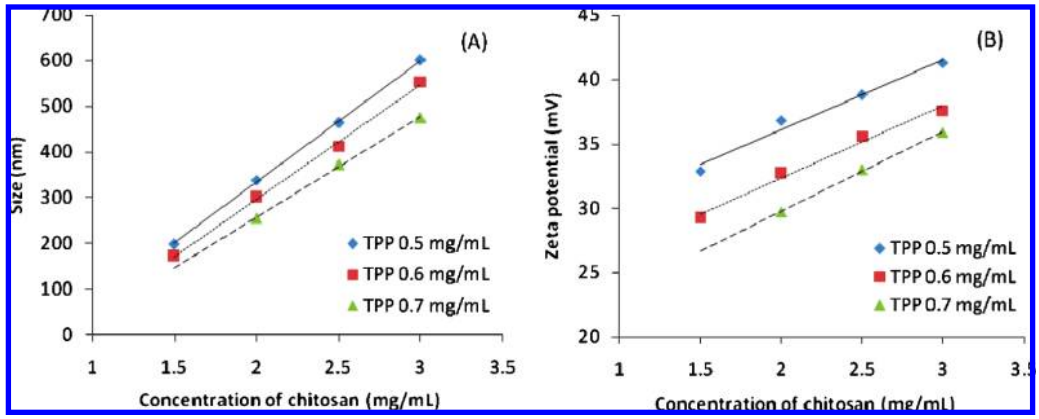

Figure 2. Particle size (**A**) and zeta potential (**B**) measurements of CS−TPP nanoparticles.

acid solution was the same as the method described above. Samples consisting of only nonloaded CS nanoparticles resuspended in each solution were used as a control. All experiments were performed in triplicate.

Changes in Properties and Release of AA-Loaded CS Nanoparticles after Heat Treatment. Three milliliters of AA-loaded CS nanoparticle solutions was transferred into 9 test tubes, and 3 test tubes were heated for 5, 10, or 15 min at 60, 80, or 100 °C, respectively. To analyze the changes in physicochemical properties for the AA-loaded CS nanoparticles after heat treatment, the particle size and zeta potential of the nanoparticles in each test tube after heat treatment were measured. The AA-loaded CS nanoparticles heated for 15 min at various temperatures were separated by centrifugation at 15000*g* and 4 °C for 30 min. The supernatant was then decanted, and the nanoparticles were resuspended in 4 mL of 0.26% acetic acid solution and kept at 37 °C for 4 days. The AA content released from nanoparticles was assessed using the release method described above. All samples were analyzed in triplicate.

RESULTS AND DISCUSSION

Physicochemical Properties of CS Nanoparticles. The preparation of CS nanoparticles is based on an ionic gelation interaction between positively charged CS and negatively charged TPP at room temperature (*11, 26*). **Figure 2A** shows the mean size of each nanoparticle suspension prepared with various CS and TPP concentrations. It demonstrates that the size of nanoparticles increased with an increase in CS and a decrease in TPP concentration, and this increase in size with concentration showed a linear relationship within the tested range. The minimum size (170 nm) of CS nanoparticles was obtained for a CS concentration of 1.5 mg/mL and a TPP concentration of 0.6 mg/mL; therefore, the ratio of CS/TPP was 2.5:1.

When CS and TPP were mixed in acetic acid solution, they spontaneously formed compact nanocomplexes with an overall positive surface charge, and the density of the surface charge was reflected in the measured zeta potential values. The zeta potential of CS–TPP nanoparticles increased linearly with increasing CS concentration and reduced with increasing TPP concentration (**Figure 2B**). This simple linear relationship could be easily explored for modulating the particle surface charge density to facilitate adhesion and transport properties of the nanoparticles.

Particle size is one of the most significant determinants in mucosal and epithelial tissue uptake of nanoparticles and in the intracellular trafficking of particles (*29*). Smaller nanoparticles (~100 nm) had a >3-fold greater arterial uptake compared to larger nanoparticles (~275 nm) in an ex vivo canine carotid artery model, because smaller nanoparticles were able to penetrate throughout the submucosal layers, whereas larger particles predominantly localized in the epithelial lining (*30, 31*). Therefore, particle size is important to enhance nanoparticle-mediated nutrient delivery, such as that of AA. AA should be entrapped in the smallest CS nanoparticles with CS of 1.5 mg/mL and TPP of 0.6 mg/mL.

Table 1. Physicochemical Properties and Encapsulation Efficiency (EE) of Ascorbic Acid (AA)-Loaded Nanoparticles as a Function of the Final AA Concentration Added to CS−TPP Nanoparticles[a]

ascorbic acid (mg/mL)	particle size (nm)	polydispersity index (μ_2/Γ^2)	zeta potential (mV)	encapsulation efficiency (%)
0.0	171.70 ± 1.18	0.343 ± 0.005	29.23 ± 0.85	0.00 ± 0.00
0.1	186.67 ± 5.44	0.369 ± 0.007	24.43 ± 0.35	11.20 ± 0.24
0.2	195.60 ± 4.18	0.387 ± 0.004	21.60 ± 0.36	12.03 ± 0.08
0.3	201.83 ± 4.51	0.400 ± 0.003	19.27 ± 0.30	10.53 ± 0.27

[a] CS 1.5 mg/mL, TPP 0.6 mg/mL. All data are mean ± standard deviation for $n = 3$ replicates.

Physicochemical Properties of AA-Loaded CS Nanoparticles and Encapsulation of AA. We selected AA as a model nutrient to investigate the feasibility of using CS nanoparticles. **Table 1** shows the size and zeta potential values of AA-loaded CS nanoparticles. The particle size and the PDI increased as the concentration of AA increased from 0.1 to 0.3 mg/mL, whereas the zeta potential reduced when the AA concentration increased.

The encapsulation of AA was demonstrated by two methods, that is, during the preparation of particles and after the formation of particles (*11*). In the first method, AA was mixed with CS solution before simultaneous cross-linking and precipitation; the acid groups of AA interact by electrostatic attraction with the positively charged amine groups of CS. AA was then loaded into cross-linked CS nanoparticles prepared by ionic gelation. In the second method, the remaining free AA was physically embedded into a matrix or absorbed onto the surface of CS nanoparticles. Consequently, it is not surprising that AA loading into internal or external CS nanoparticles leads to an increase in the size and the PDI and that the AA absorbed onto the surface of AA-loaded CS nanoparticles leads to a decrease in the positive charge of the nanoparticles.

Table 1 also shows the EE of AA into CS nanoparticles. The EE of AA maintained a fixed range (10–12%) when the AA concentration increased from 0.1 to 0.3 mg/mL. The EE of CS nanoparticles using glycyrrhetic acid (GLA) and proteins such as BSA have been shown to be about 80–90% (*12, 26*). As a result of this study, however, the encapsulation of AA into CS nanoparticles for application in food processing was harder than the encapsulation of the others. The hydrogen ion

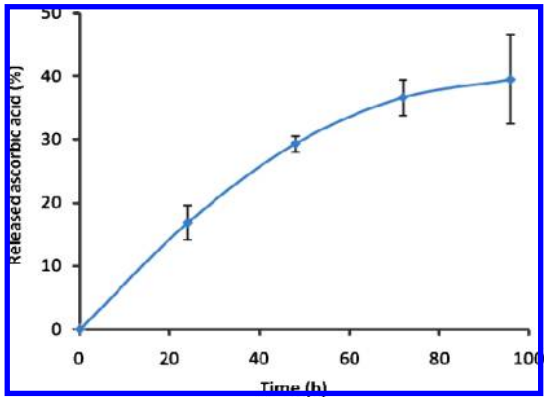

Figure 3. AA release profile from AA-loaded CS−TPP nanoparticles at 37 °C. All data are mean ± standard deviation ($n = 3$). Loaded AA = 11%, CS = 1.5 mg/mL, TPP = 0.6 mg/mL.

is regularly dissociated from AA in CS solution, and only the acid group of the dissociated AA interacts with the positively charged amine groups of the CS to form the AA-loaded CS nanoparticles.

In Vitro Release of AA from CS Nanoparticles. Figure 3 shows the release profile of AA from CS nanoparticles. The release profile of the AA-loaded CS nanoparticles exhibited a small burst of about 17% in the first 24 h and then maintained a slow and constant release rate and reached a saturated point. In the case of release from the surface of nanoparticles, absorbed AA instantaneously dissolves when it comes into contact with the release solution. This type of AA release leads to a burst of AA. He et al. (*32*) observed that cimetidine-loaded CS microspheres show a similar rapid release in the early stages of dissolution. Zhou et al. (*33*) reported that the release from microspheres involves two different mechanisms of drug molecule diffusion and polymer matrix degradation. The burst of drug is associated with drug molecules dispersing close to the microsphere surface; these molecules easily diffuse in the initial incubation time. This hypothesis is also applicable for AA release from nanoparticles. Because the size of the AA molecule is much smaller than that of the nanoparticles, AA molecules easily and rapidly diffuse through the surface or the pore of the nanoparticles. Therefore, the rapid dissolution process suggests that the released solution penetrates into the particles due to the hydrophilic nature of CS and dissolves the entrapped AA. The nanoparticles have a very large specific surface area that can absorb AA, so that the first burst release is caused in part by the AA desorbed from the nanoparticle surface.

Physicochemical Properties and Release of AA-Loaded CS Nanoparticles after Heat Treatment. Figure 4 shows the change in size and zeta potential of CS and AA-loaded CS nanoparticles during heat treatment. In the case of size and zeta potential, CS and AA-loaded CS nanoparticles at 80 and 100 °C were rapidly reduced in the first 5 min and then were slowly reduced into a regular range. These results show that the layer formed during absorption of AA into the surface of the particles in the initial heat treatment was affected by the initial heat treatment. In other words, the AA adsorbed into the surface and the cross-linking structure related to the formation of the layer were affected by heat treatment. Consequently, particle size was reduced and the positive charge on the surface was changed; hence, the zeta potential was lowered. This mechanism proceeds relatively rapidly with the rise in temperature. With further heat treatment, however, particle size and zeta potential were maintained within a regular range, probably because the matrix structure in which AA and CS were combined through ionic gelation inside the particles was more stable than the particle surface. Consequently, as in the two methods for the encapsulation of AA into particles, there are two characteristics

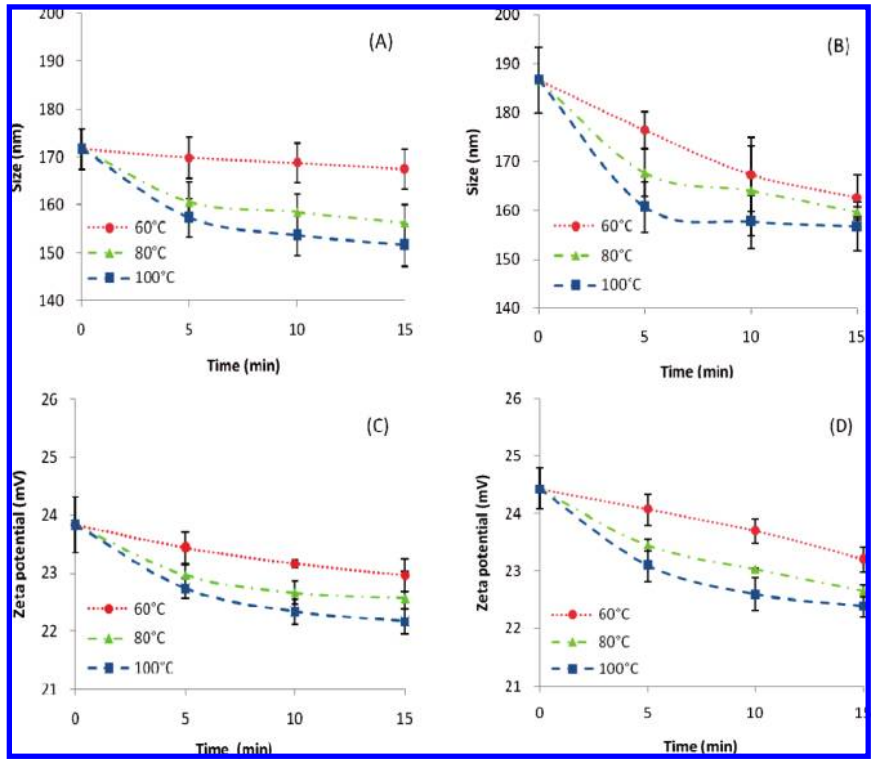

Figure 4. Comparison of the particle size (**A**, **B**) and zeta potential (**C**, **D**) of CS nanoparticles (**A**, **C**) and AA-loaded CS nanoparticles (**B**, **D**) after heat treatment at 60, 80, and 100 °C. All data are mean ± standard deviation ($n = 3$). Encapsulation efficiency = 11%, CS = 1.5 mg/mL, TPP = 0.6 mg/mL.

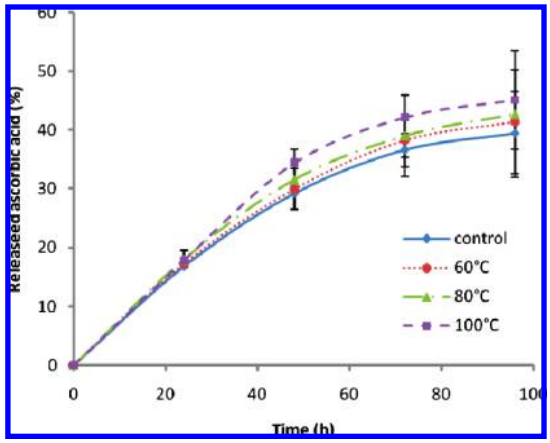

Figure 5. Comparison of the AA release profile of AA-loaded CS nanoparticles heated for 15 min at 60, 80, or 100 °C. All data are mean ± standard deviation ($n = 3$). Encapsulation efficiency = 11%, CS = 1.5 mg/mL, TPP = 0.6 mg/mL.

of the structure of which a particle is composed: the surface and the inner part. Therefore, the stability of the inner part attained through heat treatment is higher than that of the particle surface, and the stability of the surface is probably affected by the heat treatment temperature.

AA in aqueous solution rapidly decreased to about 75.5% after 15 min at 121 °C (*34*), whereas AA release from CS nanoparticles was shown to be over 40% for 4 days after heat treatment for 30 min at 100 °C (**Figure 5**). This result suggests that the stability of AA with CS nanoparticles was higher than the one of AA without CS nanoparticles during heat treatment.

When the heat treatment on equal time at various temperatures and the release effect were compared, at the beginning of release, the stability of the surface was weakened with the rise in temperature; as a result, the burst release at high temperature appeared higher (**Figure 5**). With a longer release time, the release was constantly higher, probably because the stability of the inside was also affected by heat treatment temperature. Agnihotri et al. (*11*) reported that the release of drug from CS particulate systems involves three different mechanisms: (a) release from the surface of particles, (b) diffusion through the swollen rubbery matrix, and (c) release due to polymer erosion. Kweon and Kang (*35*) reported that drug release from CS−g–poly(vinyl alcohol) matrix was controlled by the extent of PVA grafting, heat treatment, or cross-link density. Thus, the penetration of the released solution into the inside particle matrix became easier and, as a result, the swelling of the internal structure increased and the AA inside was released more quickly. Therefore, it was confirmed that the stability of AA-loaded CS nanoparticles was affected by temperature but that the internal stability was higher than the surface stability. After heat treatment at various temperatures, the release effect was high compared to that in non-heat-treated CS particles. These results of the heat stability of AA-loaded CS nanoparticles suggest their stability in application in foods and the possibility for enhancement of antioxidant effects.

In conclusion, in food processing involving heat treatment, AA is easily oxidized and lost. The applications of nanoparticles can be expanded to various types of food processing, as shown with AA-loaded CS nanoparticles, for which heat stability of the CS nanoparticles and the AA has been demonstrated. Furthermore, the results show that food supplemented with nanoparticles can overcome difficulties in the swallowing of conventional capsules. Such a nanoparticle formulation will have a long-term antioxidant effect on food rather than a temporary effect. The direct penetration of nanoparticle-containing supplements into intestinal cells will further enhance the antioxidant effects in the body. The results presented in this study clearly demonstrate the heat stability in various conditions and the possible use of AA-loaded CS nanoparticles to enhance antioxidant effects because of the continuous release and the heat stability of CS nanoparticles for AA in food processing.

LITERATURE CITED

(1) Knapczyk, J.; Krowczynski, L.; Krzck, J.; Brzeski, M.; Nirnberg, E.; Schenk, D.; Struszcyk, H. Requirements of chitosan for pharmaceutical and biomedical applications. In *Chitin and Chitosan: Sources, Chemistry, Biochemistry, Physical Properties and Applications*; Skjak-Braek, G., Anthonsen, T., Sandford, P. A., Eds.; Elsevier: London, U.K., 1989; pp 657–663.

(2) Hirano, S.; Seino, H.; Akiyama, Y.; Nonaka, I. Biocompatibility of chitosan by oral and intravenous administration. *Polym. Eng. Sci.* **1989**, *59*, 897–901.

(3) Majeti, N. V.; Kumar, R. A review of chitin and chitosan applications. *React. Funct. Polym.* **2000**, *46*, 1–27.

(4) Aspden, T. J.; Mason, J. D.; Jones, N. S. Chitosan as a nasal delivery system: the effect of chitosan solutions on in vitro and in vivo mucociliary transport rates in human turbinates and volunteers. *J. Pharm. Sci.* **1997**, *86*, 509–513.

(5) Lehr, C. M.; Bouwstra, J. A.; Schacht, E.; Junginger, H. E. *In vitro* evaluation of mucoadhesive properties of chitosan and some other natural polymers. *Int. J. Pharm.* **1992**, *78*, 43–48.

(6) Dumitriu, S.; Chornet, E. Inclusion and release of proteins from polysaccharide-based polyion complexes. *Adv. Drug Delivery Rev.* **1998**, *31*, 223–246.

(7) Takeuchi, H.; Yamamoto, H.; Niwa, T.; Hino, T.; Kawashima, Y. Enteral absorption of insulin in rats from mucoadhesive chitosan-coated liposomes. *Pharm. Res.* **1996**, *13*, 896–901.

(8) Berscht, P. C.; Nies, B.; Liebendorfer, A.; Kreuter, J. Incorporation of basic fibroblast growth factor into methylpyrrolidinone chitosan fleeces and determination of the *in vitro* release characteristics. *Biomaterials* **1994**, *15*, 593–600.

(9) Lin, Y. H.; Chung, C. K.; Chen, C. T.; Liang, H. F.; Chen, S. C.; Sung, H. W. Preparation of nanoparticles composed of chitosan/poly-γ-glutamic acid and evaluation of their permeability through Caco-2 cells. *Biomacromolecules* **2005**, *6*, 1104–1112.

(10) Suheyla, K. H. Chitosan: properties, preparations and application to microparticulate systems. *J. Microencapsulation* **1997**, *14*, 689–711.

(11) Agnihotri, S. A.; Mallikarjuna, N. N.; Aminabhavi, T. M. Recent advances on chitosan-based micro- and nanoparticles in durg delivery. *J. Controlled Release* **2004**, *100*, 5–28.

(12) Calvo, P.; Remunan-López, C.; Vila-Jato, J. L.; Alonso, M. J. Novel hydrophilic chitosan−polyethylene oxide nanoparticles as protein carriers. *J. Appl. Polym. Sci.* **1997**, *63*, 125–132.

(13) Janes, K. A.; Calvo, P.; Alonso, M. J. Polysaccharide colloidal particles as delivery systems for macromolecules. *Adv. Drug Delivery Rev.* **2001**, *47*, 83–97.

(14) Mao, H. Q.; Krishnendu, R.; Troung-Le, V. L.; Janes, K. A.; Lin, K. L.; August, J. T.; Leong, K. W. Chitosan−DNA nanoparticles as gene carriers: synthesis, characterization and transfection efficiency. *J. Controlled Release* **2001**, *70*, 399–421.

(15) Takeuchi, H.; Yamamoto, H.; Kawachima, Y. Mucoadhesive nanoparticulate systems for peptide drug delivery. *Adv. Drug Delivery Rev.* **2001**, *47*, 39–54.

(16) Pan, Y.; Li, Y. J.; Zhao, H. Y.; Zheng, J. M.; Xu, H.; Wei, G.; Hao, J. S.; Cui, F. D. Bioadhesive polysaccharide in protein delivery system: chitosan nanoparticles improve the intestinal absorption of insulin in vivo. *Int. J. Pharm.* **2002**, *249*, 139–147.

(17) Kim, T. H.; Park, I. K.; Nah, J. W.; Choi, Y. J.; Cho, C. S. Galactosylated chitosan/DNA nanoparticles prepared using water-soluble chitosan as a gene carrier. *Biomaterials* **2004**, *25*, 3783–3792.

(18) Portero, A.; Remunan-Lopez, C.; Criado, M. T.; Alonso, M. J. Reacetylated chitosan microspheres for controlled delivery of anti-

microbial agents to the gastric mucosa. *J. Microencapsulation* **2002**, *19*, 797–809.
(19) Bendich, A.; Machlin, L. J.; Scandurra, O.; Barton, G. W.; Wayner, D. D. M. The antioxidant role of vitamin C. *Adv. Free Radical. Biol. Med.* **1986**, *2*, 419–444.
(20) Bossi, A.; Piletsky, S. A.; Piletska, E. V.; Righetti, P. G.; Turner, A. P. An assay for ascorbic acid based on polyaniline-coated microplates. *Anal. Chem.* **2000**, *72*, 4296–4300.
(21) Yamamoto, I.; Tai, A.; Fujinami, Y.; Sasaki, K.; Okazaki, S. Synthesis and characterization of a series of novel monoacylated ascorbic acid derivatives, 6-*O*-acyl-2-*O*-α-D-glucopyranosyl-L-ascorbic acids, as skin antioxidants. *J. Med. Chem.* **2002**, *45*, 462–468.
(22) Eitenmiller, R. R.; Landen, W. O. Ascorbic acid. In *Vitamin Analysis for the Health and Food Sciences*; CRC Press: Boca Raton, FL, 1999; pp 223–228.
(23) Rojas, A. M.; Gerschenson, L. N. Ascorbic acid destruction in aqueous model system: an additional discussion. *J. Sci. Food Agric.* **2001**, *81*, 1433–1439.
(24) Yuan, J. P.; Chen, F. Degradation of ascorbic acid in aqueous solution. *J. Agric. Food Chem.* **1998**, *46*, 5078–5082.
(25) Gan, Q.; Wang, T.; Cochrane, C.; McCarron, P. Modulation of surface charge, particle size and morphological properties of chitosan-TPP nanoparticles intended for gene deliver. *Colloids Surf., B* **2005**, *44*, 65–73.
(26) Wu, Y.; Yang, W.; Wang, C.; Hu, J.; Fu, S. Chitosan nanoparticles as a novel deliver system for ammonium glycyrrhizinate. *Int. J. Pharm.* **2005**, *295*, 235–245.
(27) Kearney, M. C. J.; Allwood, M. C.; Martin, H.; Neal, T.; Hardy, G. The influence of amino acid source on the stability of ascorbic acid in TPN mixtures. *Nutrition* **1998**, *14*, 173–178.
(28) Yoon, H. S.; Son, Y. J.; Han, J. S.; Lee, J. S.; Han, N. S. Comparison of D- and L-lactic acid contents in commercial kimchi and sauerkraut. *Food Sci. Biotechnol.* **2005**, *14*, 64–67.
(29) Panyam, J.; Labhasetwar, V. Biodegradable nanoparticles for drug and gene delivery to cells and tissue. *Adv. Drug Delivery Rev.* **2003**, *55*, 329–347.
(30) Song, C.; Labhasetwar, V.; Cui, X.; Underwood, T.; Levy, R. J. Arterial uptake of biodegradable nanoparticles for intravascular local drug delivery: results with an acute dog model. *J. Controlled Release* **1998**, *54*, 201–211.
(31) Desai, M. P.; Labhasetwar, V.; Amidon, G. L.; Levy, R. J. Gastrointestinal uptake of biodegradable microparticles: effect of particle size. *Pharm. Res.* **1996**, *13*, 1838–1845.
(32) He, P.; Davis, S. S.; Illum, L. Chitosan microspheres prepared by spray drying. *Int. J. Pharm.* **1999**, *187*, 53–65.
(33) Zhou, S. B.; Deng, X. M.; Li, X. H. Investigation on a novel core-coated microspheres protein delivery system. *J. Controlled Release* **2001**, *75*, 27–36.
(34) Touitou, E.; Alkabes, A.; Memoli, F.; Alhaique, F. Glutathione stabilizes ascorbic acid in aqueous solution. *Int. J. Pharm.* **1996**, *133*, 85–88.
(35) Kweon, D. K.; Kang, D. W. Drug-release behavior of chitosan–poly. (vinyl alcohol) copolymer matrix. *J. Appl. Polym. Sci.* **1999**, *74*, 458–464.

Received for review November 20, 2007. Revised manuscript received January 14, 2008. Accepted January 15, 2008.

JF073385E